ChemComm

Accepted Manuscript

Volume 1 | Number 1 | Jan 2013 | Pages 1–100

ChemComm

Chemical Communications
www.rsc.org/chemcomm

ROYAL SOCIETY OF CHEMISTRY

ROYAL SOCIETY OF CHEMISTRY

www.rsc.org/chemcomm

A graphical and textual abstract

Red fluorescent luminogen from pyrrole derivatives with aggregation-enhanced emission for cell membrane imaging

Guogang Liu, Didi Chen, Lingwei Kong, Jianbing Shi, Bin Tong, Junge Zhi, Xiao Feng and Yuping Dong

A dye emitted red fluorescence with aggregation-enhanced emission properties was reported here. It can be utilized to specifically recognize the cell membrane of MCF-7 and 293T cell lines during the bio-imaging.

Journal Name
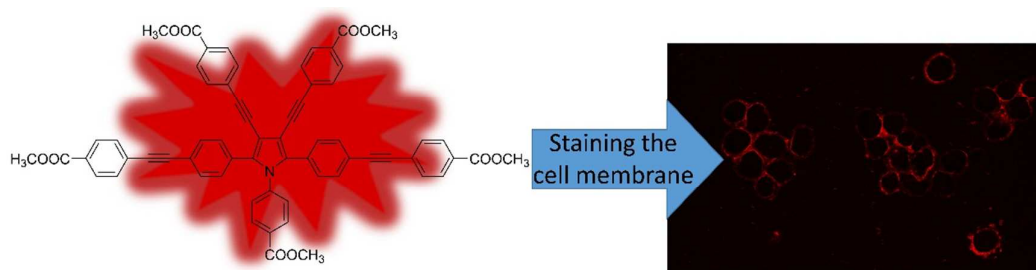
COMMUNICATION

Red fluorescent luminogen from pyrrole derivatives with aggregation-enhanced emission for cell membrane imaging

Guogang Liu,[a] Didi Chen,[a] Lingwei Kong,[a] Jianbing Shi,*[a] Bin Tong,[a] Junge Zhi,[b] Xiao Feng,[b] and Yuping Dong*[a]

A dye emitted red fluorescence with aggregation-enhanced emission properties was reported here. It can be utilized to specifically recognize the cell membrane of MCF-7 and 293T cell lines during the bio-imaging.

It is well known that the fluorescent intensity of many organic dyes weakens when their solution concentrations are increased or when they are aggregated in experimental condition, which is due to the formation of such detrimental species as excimers and exciplexes.[1] This phenomenon is commonly called aggregation-caused quenching (ACQ). This ACQ effect was particularly obvious in the applications of the fluorophores as biosensors or cell imaging agent because of their planar and rigid backbones which tend to aggregate in their aqueous practical environment.[2] A photo-physical phenomenon associated with fluorogen aggregation is aggregation-induced emission (AIE), which is opposite to the ACQ phenomenon.[3] In the AIE process, weakly fluorescent chromophores are induced to emit efficiently by the aggregation formation. A number of organic molecules with propeller-shaped structures have been found to show pronounced AIE effect, such as siloles,[4] tetraphenylethene,[5] distyrylanthracene,[6] cyano-substituted diarylethylene,[7] and aryl-substituted pyrrole derivatives.[8] The discovery of AIE molecules offers a straightforward solution to overcome the ACQ problem. Moreover, there are increasing evidences indicating that AIE dyes have highly potential in biosensor or bioimaging,[9] which have some advantages such as higher sensitivity,[10] larger signal-to-noise ratio with minimized background fluorescence,[11] and so on. Yet, most AIE fluorogens used for light-up probe or imaging agent are limited to those with either blue or green emission.[9a, 12] As a result, it is highly desirable to develop AIE dyes with long wavelength emission for cell imaging because deployment of such dyes can reduce the photo-limiting interference.[13]

One effective strategy to seek long wavelength emissive fluorophores is to combine electron rich units with deficient ones so as to form a donor (D) – acceptor (A) structure.[14] Their fluorescent intensity in strong D-A system, however, is dependent on the polarity of the environments, for example, lower fluorescent intensity in high polar media.[15] Another efficient method to get long wavelength emissive fluorophores is to increase the degree of π-conjugation, which the environmental dependence for their

fluorescence becomes lower. In our previous work, carboxylic salt of aryl-substituted pyrrole derivatives can be used for "turn-on" probe for sensitively and selectively detecting aluminium ions based on the AIE mechanism.[8b, 8c] But those pyrrole derivatives mainly emit in the blue areas, which is unfavorable for the bio-imaging. In this manuscript, therefore, we report a new compound **5** with an extended π-conjugation structure, as shown in Scheme 1. And it is also a typical D-π-A structure, which has a pyrrolyl group as the electron donor, methyl benzoate as an electron acceptor, and phenylethynyl as a π-conjugation bridge, respectively. The compound shows the red photoluminescence with the aggregation-enhanced emission (AEE) characteristics that emitted weakly in the solution but strongly in the aggregation. Furthermore, this AEE dye can be applied in the cell imaging, specifically for the membrane of MCF-7 and 293T cell lines.
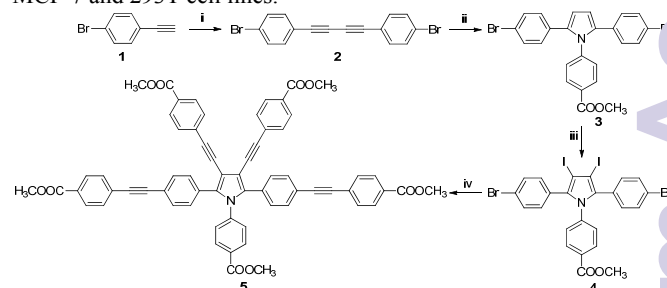
Scheme 1. Synthesis route of target compound **5**. (i) CuCl/TMEDA/O₂, 50°C; (ii) methyl 4-aminobenzoate, reflux; (iii) ICl/NaHCO₃, r.t.; (iv) methyl 4-ethynylbenzoate/PdCl₂(PPh₃)₂/CuI/PPh₃, 65°C.

The compound **5** was prepared by the synthetic route as shown in Scheme 1. The oxidative coupling reaction of 1-bromo-4-ethynylbenzene (**1**) gave 1,4-di(4-bromophenyl)-butadiyne (**2**) in 89% yield. The pyrrole derivative (**3**) was synthesized by reaction of **2** and methyl 4-aminobenzoate in the moderate yield (56%). Iodination of compound **3** using ICl afforded di-iodinated the pyrrole derivative **4** in good yield (83%). The Sonogashira cross-coupling reaction of compound **4** with methyl 4-ethynylbenzoate gave the target product **5** in 28% yield. All compounds were fully

characterized by spectroscopic methods, see the electronic supplementary information (ESI) for details.

We first studied the absorption and photoluminescence (PL) spectra of **5** in some solvents with different polarities (dielectric constant (ε)). As shown in Fig. S1a, the absorption bands from 275 to 400 nm are attributed to π–π* transitions of the conjugated aromatic segments, whereas those at longer wavelength from 400 to 600 nm are due to the intramolecular charge transfer between the donor and acceptor. It can be found that the longer absorption peak is located at 455 nm in hexane while others are located between 465 and 470 nm in the rest of seven solvents. Moreover, the emission in hexane shows the strongest intensity in these eight solvents and the shortest in emissive maximum located at 577 nm, as shown in Fig. S1b, which is blue-shifted 10 nm or more than others. Except for hexane, there are no obvious changes in the absorption or emission maximum although those solvents are big differences in ε. In D-A system, the absorption or emission is more or less dependent of solvent polarity. But for the pyrrole derivative **5**, it is insensitive to the environmental polarity based on the above fluorescence and absorption results of different solvent response. This represents an advantage for some applications such as bio-imaging because there is different polarity in the different organelle of cell.

Many fluorescent dyes aggregate when dispersed in aqueous media or bound to biological media in large quantities. Compared to traditional ACQ dyes, AIE dyes can emit efficiently by the aggregation formation. Dye **5** is soluble in common solvents such as DCM, THF and AN but insoluble in water. Dilute solutions of **5** in THF are weakly emissive. Addition of non-solvent water into its THF solution can quickly enhance the emission when the water fraction exceeds 60% because of aggregation formation, as shown in Fig. 1a. The fluorescent intensity of dye **5** is increased by approximately 7 fold when the water fraction reached 80% along with a slight 10 nm red-shift from 593 nm to 603 nm. Its emission decreased slightly when the water fraction exceeded 80%, see the inset of Fig. 1a. The track of the transmittance of different water fraction showed that the nanoparticles were formed when f_w became higher than 60%, which transmittance is obvious reduced as shown in Fig. S2a (see ESI). The dynamic light scattering (DLS) further confirmed the aggregation formation, and its particle diameter sizes were 108.5 and 65.2 nm at the water fraction 80% and 99%, respectively, as shown in Figs. S3a and S3b in ESI. If non-solvent hexane, a nonpolar solvent, is used, the enhanced intensity of **5** reached 9-fold when f_H reached 99% along with an obvious blue-shift from 593 to 580 nm (Fig. 1b). The transmittance of them is almost the same (Fig. S2b in ESI) but DLS results indicated that nanoparticles were also formed and their sizes are approximately 15.6 nm (Fig. S3c in ESI), which have no effect on the transmittance. Evidently, the enhanced emission of **5** is induced by the aggregation formation, or in other words, **5** is AEE–active. Additionally, the quantum yield (Φ) is the important parameter for a fluorophore, and the emission efficiency can be quantitatively evaluated accordingly. The absolute PL quantum yields of **5** in both solution and solid states were determined by using an integrating sphere. The Φ values of 5 in THF solution and solid state were 0.88% and 5.44%, respectively.

Moreover, the Φ values of **5** in the aggregate by the addition of water (f_w = 99%) or hexane (f_H = 99%) were 5.71% and 4.29% respectively. The result is in good agreement with the above discussion. That is, it is a typical AEE dye with a satisfactory emission efficiency in solid state compared with other reported red emission dyes.[16]
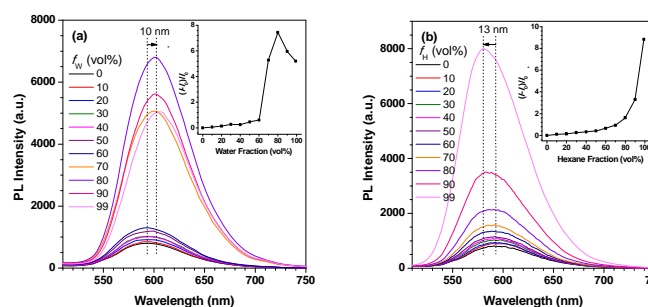

Fig. 1 PL spectra of **5** in the (a) THF-water and (b) THF-hexane mixtures with different water or hexane fraction. [**5**] = 10 μM; Excitation wavelength: 470 nm. Insert: Correlation between the net increase in PL intensity [$(I-I_0)/I_0$] of **5** and water or hexane fraction.

To gain a better understanding of this optical property at the molecular level, density functional theory calculations were carried out using a suite of Gaussian 09 program. The nonlocal density functional of B3LYP with 6-31G (d) basis sets was used for the computation. Fig. 2 shows the optimized structures, orbital distributions of the highest occupied molecular orbital (HOMO) and lowest unoccupied molecular orbital (LUMO) of **5**. The conformation of **5** in the monomolecular state is flexible and twisted according to the optimized structure (Fig. 2a), which is difficult to pack in a highly ordered fashion. Actually, we attempted a variety of methods to grow single crystals of **5** but all failed. This seems to be a hint that the emission enhancement was not attributed to the J-aggregation during the aggregation formation. For a D-A system, the process of twisted intramolecular charge transfer (TICT) often occurred. But TICT is very sensitive to the change of environment, particularly the polarity variation. For example, 1,4-bis[1-cyano-(4-(diphenylamino)phenyl)vinyl]benzene is composed of two pairs of D-A units and exhibited a marked solvatochromic effect in solution with its emission red-shifting from green (λ_{em} = 510 nm) in hexane to red (λ_{em} = 667 nm) in DMF.[17] But for this pyrrole derivative **5**, it is insensitive to the solvent polarity in solution as the above-mentioned discussion, which can be inferred that the weaker emission of **5** in solution is not predominately controlled by TICT. The calculated result of LUMO demonstrated that the electron density is mainly centered on the pyrrole core and 1,2,5-position substituted groups (Fig. 2c), and no obvious charge separation was observed between the donor and acceptor units. These results can presumably exclude the possibility that the emission enhancement in the aggregation state is originated from the inhibition of the TICT process. From the above discussion on optical properties and theoretical calculation, it can be concluded that the restriction of intramolecular rotation or motion is the major factor for the AEE phenomena observed in the twisted conformation of **5**. Based on the DFT calculations, compared to its HOMO, there are greatly

extended the conjugation degree in the LUMO because the electronic clouds evenly distributed on the pyrrolyl core, 1-postion methyl benzoate, 2,5-position 4-{2-[(4-methoxycarbonyl)phenyl] ethynyl}phenyl, and 3,4-postion ethynyl groups, which are very big conjugated systems and thus led to the red emission. Moreover, it is noteworthy noting that there is a good electron delocalization in the ethynyl groups whether HOMO or LUMO, which indicates that triple bond may serve as a good π–bridge for the charge motion in D-π-A system.

exhibits low cytotoxicity. Even the concentration reached 25 μM, the cell viability remained above 90% after 24 h, which confirmed the good biocompatibility of dye **5**. Simultaneously, the data of apoptosis of MCF-7 and 293T cells further show little influence on cell viability. As shown in Fig. S7, there are no obvious early apoptosis and death in MCF-7 cells or 293T cells for 6 h and 24 h incubation with 10 μM of dye **5**. Therefore, this AEE dye is expected to be a promising candidate for cellular membrane imaging with some such advantages as AEE characteristic, intense red emission and excellent biocompatibility.
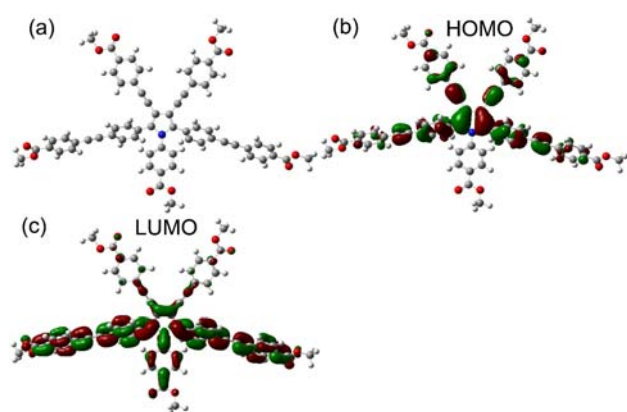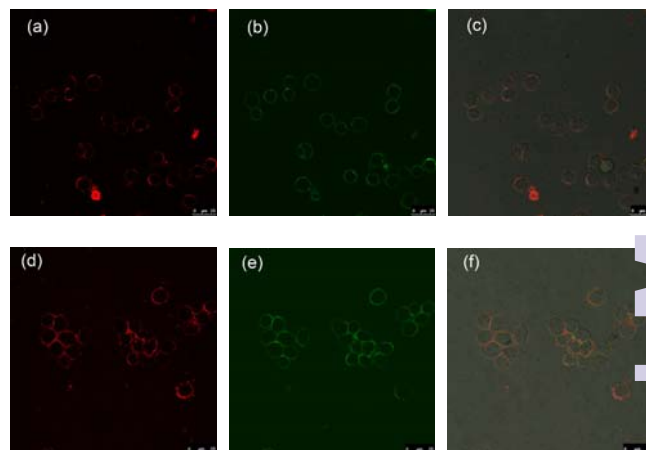

Fig. 2 (a) The optimized structure of **5** and (b) its molecular orbital amplitude plot of HOMO and (c) that of LUMO calculated using B3LYP/6-31G basis set with G09 program.

Fig. 3 CLSM images of living MCF-7 (a-c) and 293T (d-f) cells treated with 10 μM solution of dye **5** for 10 min at 37 ᵒC. The cells were pre-stained with commercial cellular membrane staining dye DiO (10 nM) for 15 min at 37 ᵒC. (a) and (d) are excited at 543 nm with a filter of 555-700 nm; (b) and (e) are excited at 488 nm with a filter of 500-535 nm; (c) and (f) are their merged pictures with bright field image.

Due to its red emission, dye **5** is therefore used as a fluorescent probe for live cell imaging. Human breast cancer cells (MCF-7 cells) and human embryonic kidney cells (293T cells) were chosen as the model cell-lines for the fluorescence imaging study by confocal laser scanning microscopy (CLSM). As shown in Fig. 3, intense red fluorescence could be observed on the cell membrane of MCF-7 and 293T cells after incubating for 10 min with 10 μM of dye **5**, respectively, upon excitation at 543 nm with red fluorescence signals collected 555-700 nm. There are almost no uptake inside the cells such as cytoplasm and other organelles. Even the incubation time is increased to 120 min, it is still targeting on the cell membranes, as shown in Fig. S4 (ESI). It is indicated that this dye can be specific staining for cell membranes. This selectivity for cell membranes is presumably originated from the interaction between methyl benzoate groups and phospholipids which are a major component of cell membranes. In addition, dye **5** shows the similar photostability in comparison with DiO after a continuous irradiation for 60 min, as shown in Fig. S5 (ESI). The signal loss of dye **5** and DiO is about 57% and 53%, respectively. After irradiation for 120 min, the residue signals are about 27% and 10% for dye **5** and DiO, respectively, which indicates that photostability of dye **5** is superior to that of DiO during the long time irradiation. To probe the cytotoxicity of **5**, the viabilities of these two cell lines were evaluated by the 3-(4,5-dimethylthiazol-2-yl)-5-(3-carboxymethoxyphenyl)-2-(4-sulfophenyl) -2H-tetrazolium (MTS) assay. We probed the influence at concentrations of 5, 10, 25, 50 and 100 μM following 6 and 24 hours of the incubation. As shown in Fig. S6 in the ESI, the results of cytotoxicity testing indicate that dye **5**

In conclusion, we designed and synthesized a new red fluorescent dye with the AEE feature. The fluorophore has a D-π-A structure but is insensitive to the environmental polarity, which allows us to take advantage of the stability to stain the living cells. More importantly, the triple bond used for π-bridge can extend the conjugation and coplanarity, which is beneficial for red emission. This red dye is specifically targeted for the imaging of cellular membrane with excellent biocompatibility. Our results thus provide a general molecular design principle to develop red fluorescent probes for the cellular imaging.

Notes and references

ᵃ School of Materials Science and Engineering, Beijing Institute of Technology, Beijing 100081, China
E-mail: bing@bit.edu.cn; chdongyp@bit.edu.cn

b School of Chemistry, Beijing Institute of Technology, Beijing 100081, China

1 (a) Y. N. Teo and E. T. Kool, *Bioconjugate Chem.*, 2009, **20**, 2371; (b) D. J. Stewart, M. J. Dalton, R. N. Swiger, T. M. Cooper, J. E. Haley and L.-S. Tan, *J. Phys. Chem. A*, 2013, **117**, 3909.

2 (a) I. B. Kim, J. N. Wilson and U. H. F. Bunz, *Chem. Commun.*, 2005, 1273; (b) I. B. Kim, H. Shin, A. J. Garcia and U. H. F. Bunz, *Bioconjugate Chem.*, 2007, **18**, 815; (c) C. Xue, F. Cai and H. Liu, *Chem.-Eur. J.*, 2008, **14**, 1648.

3 (a) J. D. Luo, Z. L. Xie, J. W. Y. Lam, L. Cheng, H. Y. Chen, C. F. Qiu, H. S. Kwok, X. W. Zhan, Y. Q. Liu, D. B. Zhu and B. Z. Tang, *Chem. Commun.*, 2001, 1740; (b) Y. Hong, J. W. Y. Lam and B. Z. Tang, *Chem. Commun.*, 2009, 4332; (c) Y. Hong, J. W. Y. Lam and B. Z. Tang, *Chem. Soc. Rev.*, 2011, **40**, 5361; (d) J. Mei, Y. Hong, J. W. Y. Lam, A. Qin, Y. Tang and B. Z. Tang, *Adv. Mater.*, 2014, **26**, 5429.

4 (a) J. W. Chen, C. C. W. Law, J. W. Y. Lam, Y. P. Dong, S. M. F. Lo, I. D. Williams, D. B. Zhu and B. Z. Tang, *Chem. Mater.*, 2003, **15**, 1535; (b) L. R. Xu, Y. Li, S. H. Li, R. R. Hu, A. J. Qin, B. Z. Tang and B. Su, *Analyst*, 2014, **139**, 2332; (c) L. Chen, Y. B. Jiang, H. Nie, P. Lu, H. H. Y. Sung, I. D. Williams, H. S. Kwok, F. Huang, A. J. Qin, Z. J. Zhao and B. Z. Tang, *Adv. Funct. Mater.*, 2014, **24**, 3621; (d) B. Chen, H. Nie, P. Lu, J. Zhou, A. J. Qin, H. Y. Qiu, Z. J. Zhao and B. Z. Tang, *Chem. Commun.*, 2014, **50**, 4500.

5 (a) Y. Q. Dong, J. W. Y. Lam, A. J. Qin, J. Z. Liu, Z. Li and B. Z. Tang, *Appl. Phys. Lett.*, 2007, **91**, 011111; (b) Q. Chen, D. Q. Zhang, G. X. Zhang, X. Y. Yang, Y. Feng, Q. H. Fan and D. B. Zhu, *Adv. Funct. Mater.*, 2010, **20**, 3244; (c) Z. J. Zhao, C. M. Deng, S. M. Chen, J. W. Y. Lam, W. Qin, P. Lu, Z. M. Wang, H. S. Kwok, Y. G. Ma, H. Y. Qiu and B. Z. Tang, *Chem. Commun.*, 2011, **47**, 8847; (d) X. B. Du, J. Qi, Z. Q. Zhang, D. G. Ma and Z. Y. Wang, *Chem. Mater.*, 2012, **24**, 2178; (e) Y. F. Dong, W. L. Wang, C. W. Zhong, J. B. Shi, B. Tong, X. Feng, J. G. Zhi and Y. P. Dong, *Tetrahedron Lett.*, 2014, **55**, 1496; (f) Y. Zhang, D. Li, Y. Li and J. Yu, *Chem. Sci.*, 2014, **5**, 2710.

6 (a) J. T. He, B. Xu, F. P. Chen, H. J. Xia, K. P. Li, L. Ye and W. J. Tian, *J. Phys. Chem. C*, 2009, **113**, 9892; (b) H. Y. Li, Z. G. Chi, B. J. Xu, X. Q. Zhang, X. F. Li, S. W. Liu, Y. Zhang and J. R. Xu, *J. Mater. Chem.*, 2011, **21**, 3760; (c) B. Xu, J. B. Zhang, S. Q. Ma, J. L. Chen, Y. J. Dong and W. J. Tian, *Prog. Chem.*, 2013, **25**, 1079; (d) L. Y. Bu, M. X. Sun, D. T. Zhang, W. Liu, Y. L. Wang, M. Zheng, S. F. Xue and W. J. Yang, *J. Mater. Chem. C*, 2013, **1**, 2028; (e) X. Li, K. Ma, H. G. Lu, B. Xu, Z. L. Wang, Y. Zhang, Y. J. Gao, L. L. Yan and W. J. Tian, *Anal. Bioanal. Chem.*, 2014, **406**, 851.

7 (a) Y. P. Li, F. Li, H. Y. Zhang, Z. Q. Xie, W. J. Xie, H. Xu, B. Li, F. Z. Shen, L. Ye, M. Hanif, D. G. Ma and Y. G. Ma, *Chem. Commun.*, 2007, 231; (b) B. Wang, Y. C. Wang, J. L. Hua, Y. H. Jiang, J. H. Huang, S. X. Qian and H. Tian, *Chem.-Eur. J.*, 2011, **17**, 2647; (c) H. T. Zhou, W. Huang, L. Ding, S. Y. Cai, X. Li, B. Li and J. H. Su, *Tetrahedron*, 2014, **70**, 7050.

8 (a) X. Feng, B. Tong, J. Shen, J. Shi, T. Han, L. Chen, J. Zhi, P. Lu, Y. Ma and Y. Dong, *J. Phys. Chem. B*, 2010, **114**, 16731; (b) T. Han, X. Feng, B. Tong, J. Shi, L. Chen, J. Zhi and Y. Dong, *Chem. Commun.*, 2012, **48**, 416; (c) X. Y. Shi, H. Wang, T. Y. Han, X. Feng, B. Tong, J. B. Shi, J. G. Zhi and Y. P. Dong, *J. Mater. Chem.*, 2012, **22**, 19296; (d) T. Y. Han, X. Feng, J. B.

Shi, B. Tong, Y. F. Dong, J. W. Y. Lam, Y. P. Dong and B. Z. Tang, *J. Mater. Chem. C*, 2013, **1**, 7534.

9 (a) D. Ding, K. Li, B. Liu and B. Z. Tang, *Acc. Chem. Res.*, 2013, **46**, 2441; (b) Z. G. Song, Y. N. Hong, R. T. K. Kwok, J. W. Y. Lam, B. Liu and B. Z. Tang, *J. Mater. Chem. B*, 2014, **2**, 1717; (c) L. Y. Wang, L. L. Yang and D. R. Cao, *Curr. Org. Chem.*, 2014, **18**, 1028.

10 (a) Z. Zhu, L. Xu, H. Li, X. Zhou, J. Qin and C. Yang, *Chem. Commun.*, 2014, **50**, 7060; (b) Y. Guo, X. Tong, L. Ji, Z. Wang, H. Wang, J. Hu and J. Pei, *Chem. Commun.*, 2015, **51**, 596.

11 (a) E. Zhao, H. Deng, S. Chen, Y. Hong, C. W. T. Leung, J. W. Y. Lam and B. Z. Tang, *Chem. Commun.*, 2014, **50**, 14451; (b) F. Hu, Y. Y. Huang, G. X. Zhang, R. Zhao, H. Yang and D. Q. Zhang, *Anal. Chem.*, 2014, **86**, 7987.

12 X. Wang, J. Hu, G. Zhang and S. Liu, *J. Am. Chem. Soc.*, 2014, **136**, 9890.

13 (a) J. V. Frangioni, *Curr. Opin. Chem. Biol.*, 2003, **7**, 626; (b) S. A. Hilderbrand and R. Weissleder, *Curr. Opin. Chem. Biol.*, 2010, **14**, 71; (c) M. A. Pysz, S. S. Gambhir and J. K. Willmann, *Clin. Radiol.*, 2010, **65**, 500.

14 (a) K. R. J. Thomas, J. T. Lin, M. Velusamy, Y.-T. Tao and C.-H. Chuen, *Adv. Funct. Mater.*, 2004, **14**, 83; (b) X. B. Du and Z. Y. Wang, *Chem. Commun.*, 2011, **47**, 4276.

15 G. L. Gibson, T. M. McCormick and D. S. Seferos, *J. Am. Chem. Soc.*, 2012, **134**, 539.

16 (a) R. Yoshii, A. Hirose, K. Tanaka and Y. Chujo, *J. Am. Chem. Soc.*, 2014, **136**, 18131; (b) Z. Tao and Y. Qian, *Chin. J. Org. Chem.*, 2014, **34**, 2354; (c) K. Namba, A. Osawa, A. Nakayama, A. Mera, F. Tano, Y. Chuman, E. Sakuda, T. Taketsugu, K. Sakaguchi, N. Kitamura and K. Tanino, *Chem. Sci.*, 2015, **6**, 1083.

17 H.-H. Fang, Q.-D. Chen, J. Yang, H. Xia, B.-R. Gao, J. Feng, Y.-G. Ma and H.-B. Sun, *J. Phys. Chem. C*, 2010, **114**, 11958.